Appl Compos Mater (2009) 16:83–92
DOI 10.1007/s10443-008-9077-z

Oxidation Behavior of C/SiC Composite with CVD SiC-B_4C Coating in a Wet Oxygen Environment

Wenbin Yang · Litong Zhang · Laifei Cheng · Yongsheng Liu · Laifei Cheng · Weihua Zhang

Received: 12 October 2008 / Accepted: 18 December 2008 /
Published online: 27 January 2009

Abstract A two-layered self healing coating with a B_4C internal layer and a SiC external layer is prepared on C/SiC composite by chemical vapor deposition (CVD). Microstructure and component of the coating was analyzed by SEM, EDS, and XRD. Oxidation behavior of SiC-B_4C coated C/SiC composite was compared with SiC-SiC coated C/SiC in an environment of $P_{H_2O}/P_{O_2}/P_{Ar} = 14/8/78$ at 700°C, 1,000°C and 1,200°C for 100 h, respectively. It is demonstrated that the SiC-B_4C coating is more efficient to protect the composite from oxidation than SiC-SiC coating below 1,000°C due to the self healing behavior. After oxidized at 700°C for 100 h, the residual flexural strength of SiC-B_4C coated C/SiC is about 86%, and that of SiC-SiC coated is about 64%. While after oxidized at 1,200°C, the former is about 86% and the later is about 89%. This is due to the enhanced evaporation of B_2O_3 at higher temperature.

Keywords Oxidation behavior · Self healing · Coating · Chemical vapor deposition · Boron carbide · Residual strength

1 Introduction

Continuous carbon fiber reinforced silicon carbide matrix composites (C/SiC) are potential candidates for a variety of applications in the aerospace field including rocket nozzles, aeronautic jet engines and aircraft braking systems [1–5]. However, the matrix cracks resulted from the mismatch of coefficient of thermal expansion (CTE) between the fiber and matrix are unavoidable [6]. These cracks remain open below matrix depositing temperature (usually 1,000°C), through which, the carbon fibers and pyrolytic carbon (PyC) interphase will be consumed by the oxidizing medium. This drawback limits long-term applications of

W. Yang · L. Zhang (✉) · L. Cheng · Y. Liu · L. Cheng · W. Zhang
National Key Laboratory of Thermostructure Composite Materials,
Northwestern Polytechnical University, Xi'an, Shaanxi 710072, People's Republic of China
e-mail: zhangyoung00@sohu.com

W. Yang
e-mail: wenbinyoung@gmail.com

C/SiC in high-temperature oxidizing environments [3, 4]. As a result, the development of reliable oxidation-resistant coating is crucial to utilizing the full potential of the composites. The oxidation of CVD SiC is passive up to 1,700°C and the formed SiO_2 film has a low oxygen diffusion coefficient. Thus CVD SiC is the fundamental coating material for oxidation protection of thermal structural composites [7]. While, researches on CVD SiC coating showed that cracks resulted from CTE mismatch between composite and coating is also unavoidable [6]. During oxidation, boron bearing materials, such as boron [8], boron doped carbon (BC_x) [3, 9–12], and B_4C [13–15] formed fluid oxide phases (B_2O_3 or B–Si–O ternary phase) which can fill cracks and slow down the in-depth diffusion of moisture and oxygen [3, 9]. So, boron-containing materials were widely used as internal layer together with CVD SiC as external layer to form a self healing multilayered coating.

Some studies on oxidation behavior of C/SiC coated with boron-containing hybrid coating have been performed. It is proved that the SiC-B-SiC coating was not suitable as oxidation protection coating for C/SiC composite up to 1,300°C in static air [8]. The results of oxidation of 3D C/SiC composites coated with SiC-graphitic (B-C)-SiC coating showed that this coating could provide oxidation protection in air up to 1,300°C for 15 h [11]. The oxidation behavior of SiC–B_4C–SiC coating protected C/C composite was in static air at 1,300°C for 200 h and showed a residual strength of about 33% [16]. These researches focused on with the oxidation in air. While, previous studies showed that water vapor can not only remarkably accelerate the volatilization of B_2O_3, but also reduce its viscosity [17–19]. This phenomenon will reduces the self-sealing ability of the boron containing self healing multilayered coating system in water vapor containing atmosphere. In the combustion process, substantial amounts of water vapor are produced from burning hydrocarbon fuels in air. Calculation showed that under equilibrium conditions 5–10% of the combustion gas is water vapor [20]. Oxidation behaviors of boron containing self healing multilayered coating in wet oxygen atmosphere are therefore a concern.

In this paper, an amorphous boron carbide coating was synthesized by CVD. The atom ratio of boron to carbon is about 4, so the deposited boron carbon material is denoted by B_4C. The CVD B_4C was used as internal layer of a SiC-B_4C multilayered coating. Firstly, the morphology and composition of the SiC-B_4C coating was reported. Then the oxidation behavior of the SiC-B_4C coating protected 3D C/SiC composite was investigated in environment of $P_{H_2O}/P_{O_2}/P_{Ar} = 14/8/78$ with a slow gas flow rate of 2.8 cm s^{-1} at 700°C, 1,000°C and 1,300°C for 100 h, respectively.

2 Experiment Procedure

2.1 Fabrication of Specimens

The detailed fabrication processes of the substrates were described in reference [11]. Two kinds of specimens were prepared. The first kind was coated with two layers of CVD SiC, denoted by SiC-SiC coating. The second kind was coated with a multilayered coating which consisted of a layer of CVD SiC as external coating and a layer of B_4C as internal coating, denoted as SiC-B_4C coating. The conditions for CVD SiC were the same as that of the SiC matrix except for the deposition time, which was 30 h each time. The CVD B_4C layer was deposited from BCl_3–CH_4–H_2 mixtures, the deposition temperature was 980°C, the pressure was 3 KPa, and the molar ratio of BCl_3 to CH_4 to H_2 was 5/1/5. During the deposition of B_4C, argon with the same velocity of flow as H_2 was used as the dilute gas to get more uniform deposition.

2.2 Oxidation Tests

The oxidation tests were conducted in a $MoSi_2$ furnace in a wet oxygen environment of $P_{H_2O}/P_{O_2}/P_{Ar} = 14/8/78$, the flowing velocity of gaseous mixtures is about 2.8 cm s^{-1}. The oxidation tests were performed at 700°C, 1,000°C, and 1,200°C for 100 h, respectively. For each experimental condition, five specimens were tested. The specimens were introduced in the furnace at desired temperature. After oxidized for a certain time, the specimens were picked out and weighted. The weight were recorded after 1, 3, 6 and 10 h for the initial 10 h, then the interval record time was 10 h until oxidized for 100 h. The specimens were measured using an electronic balance with a sensitivity of 0.01 mg (METTLER TOLEDO AG 135).

2.3 Measurements of the Composites

The surface and fracture section morphologies of the coatings were observed with a scanning electron microscope (SEM, SMJ-6700). An energy dispersive X-ray spectrum (EDS, EDXA) was performed to identify the element content of boron and carbon in the multilayereded coating. The EDS was calibrated with a B_4C standard (99.5%, CERAC, USA) before the quantitative analysis of the deposited B_4C coating. Phase identification was obtained with an X-ray diffraction device (XRD, Rigaku D/MAX-2400 with Cu K*a* radiation) in grazing incidence (GIXRD) mode.

Flexural strength of the specimens before and after oxidation was measured by a three-point bending method at room temperature. The span dimension was 20 mm and the loading rate was 0.5 mm·min^{-1}.

3 Results and Discussion

3.1 Characterization of the as Received SiC-B_4C Coating

Figure 1 shows the surface morphology and EDS result of as received B_4C layer. It is clear that the B_4C layer has typical cauliflower-like surface which indicates that the B_4C is deposited by direct nucleation from liquid phase. The EDS analysis exhibits only boron and

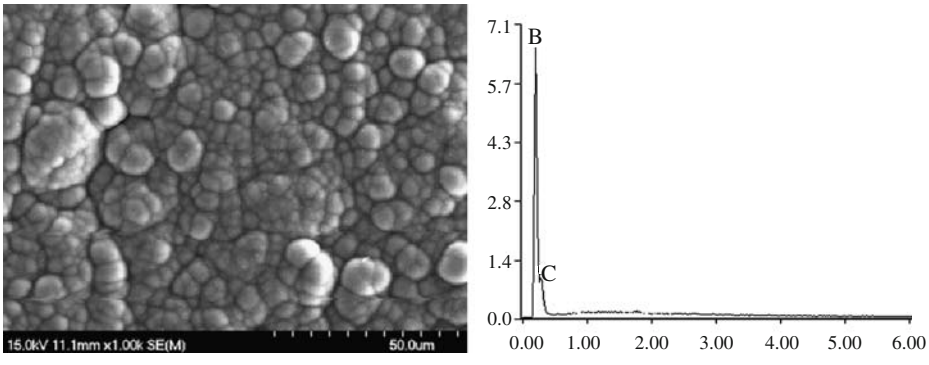

Fig. 1 Characterizations of the CVD B_4C layer showing, **a** surface morphology; **b** EDS pattern

Table 1 The elements and content (EDS) of the CVD B4C layer

Element	Wt. %	At. %
B	80	82
C	20	18

carbon peaks, which contents are given in Table 1. It can be seen that the atom ratio of boron to carbon is about 4, so the deposited boron carbon materials shall be denoted by B_4C. The XRD analysis found no evidence of either boron carbide crystal or graphite phase. This means that the deposited B_4C is amorphous, which is consistent with other previous results [21, 22].

Figure 2 shows the fracture section of the SiC-B_4C coating, in which, the B_4C layer exhibits dense glass-like fracture section morphology. The thickness of B_4C layer is about 18 μm, and that of the external SiC layer is about 25 μm. Figure 3 shows that the cracks are deflected at the interfaces of the SiC-B_4C coating. This phenomenon will prolong the diffusion path of the corrosive atmosphere before it reaches the carbon fiber.

Figure 4 shows the surface crack density of SiC-SiC coating and SiC-B_4C coating, it is clear that the crack density of SiC coating is about twice that of SiC-B_4C coating. This may due to the less adhesion at the heterogeneous interfaces of the SiC-B_4C coating, shown in Fig. 3, which not only released thermal stress but also weakened transfer of the thermal stress.

3.2 Morphologies and Compositions of Hybrid Coating after Oxidation

Figure 5 shows the morphologies of the SiC-B_4C coatings after oxidation at 700°C for 100 h. It is clear that the external SiC layer of the specimen keeps intact and there is no evidence of liquid phase around crack. After oxidation at 1000°C, as shown in Fig. 6, the outer SiC layer is homogeneously covered with a layer of dense but rimous glass with a thickness of about 1.7 μm. There are two kinds of cracks in the glass layer, namely the long straight crack partly healed by liquid phase balls, and the direction free net cracks. The EDS result of the ramous glass layer showed that this layer consisted of Si, O, and C. Therefore, it can be deduced that the glass layer is SiO_2, and the carbon signal is from SiC beneath the SiO_2 layer. While the EDS result of liquid balls showed Si, O, and B, which indicated that the liquid balls consisted of B_2O_3.

Based on the microstructure and EDS analysis, it can be deduced that the long straight crack is a coating crack which deduced by the CET mismatch between coating and composite. During oxidation at 1000°C, the coating crack was nearly closed, however, the wet oxygen gas still can reach the internal B_4C layer. The liquid B_2O_3 was formed by oxidation of B_4C accompanied by a remarkable volume increase [23], which makes it

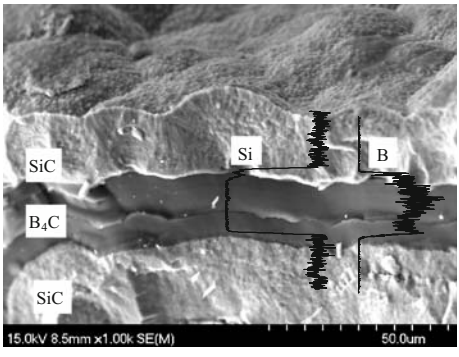

Fig. 2 Fracture section morphology and EDS line scan of the SiC-B_4C coating

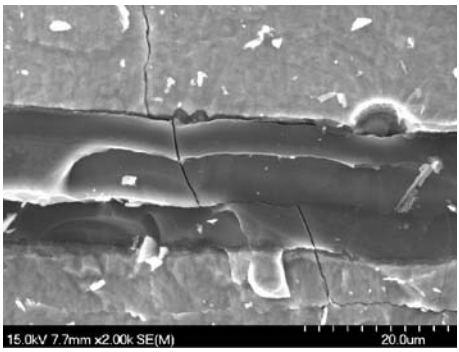

Fig. 3 Crack deflections at interfaces of the SiC-B_4C coating

overflowed from the crack of external SiC layer and formed a series of liquid balls above the crack. During cooling stage, the crack was re-ruptured and the tension stress also torn the glass phase balls. On the same time, accelerated oxidation of SiC in wet oxygen atmosphere leads to the surface of coating was covered by a thin layer of SiO_2 [24, 25]. During cooling-down, volume contraction of SiO_2 resulted in the net cracks produced all over the glass layer.

Figure 7 shows the surface morphologies and EDS analysis of the SiC-B_4C coatings after oxidation at 1,200°C for 100 h. It is clear that the specimen is covered by a layer of rimous SiO_2. Bubbles and partial peel-off can be observed in the SiO_2 layer and cracks also can be found in the exposed underlayer. The EDS analysis of the underlayer shows Si, O, and C, which indicates that beneath the surface rimous SiO_2 layer, there is still a layer of SiO_2. Magnified image of the surface SiO_2 is shown in Fig. 7b, it is clear that the surface SiO_2 layer exhibits a distinct dendrite morphology, which indicates the crystallization of the SiO_2 layer. The GIXRD patterns of the SiC- B_4C coatings after oxidation for 100 h are shown in Fig. 8. It is clear that the SiO_2 crystallized after oxidation at 1,000°C and the crystallization was enhanced after oxidation at 1,200°C.

Figure 9 shows the cross section of the SiC-B_4C coatings after oxidation at 1,200°C for 100 h. The partial enlarged detail of the glass layer exhibited distinct two kinds of structures. The external layer is about 1.5 μm and shows a dense fracture structure, while the internal layer shows a porous structure. This may due to the diffusion coefficient of water in silica is an order of magnitude smaller than that of oxygen. However, the solubility

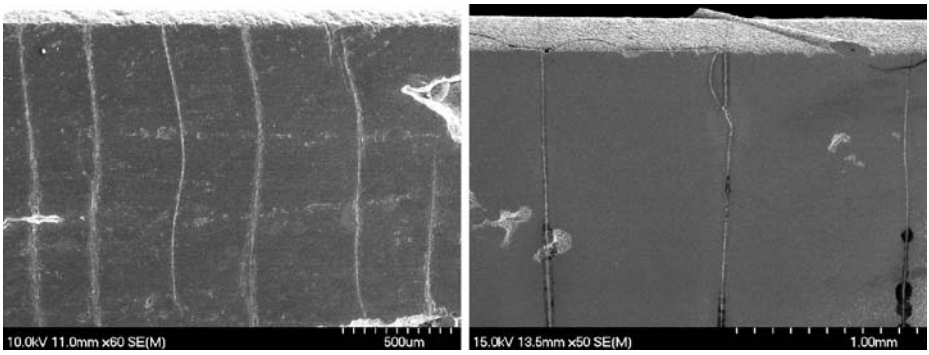

(a) (b)

Fig. 4 Surface crack density of **a** SiC-SiC coating and **b** SiC-B_4C coating

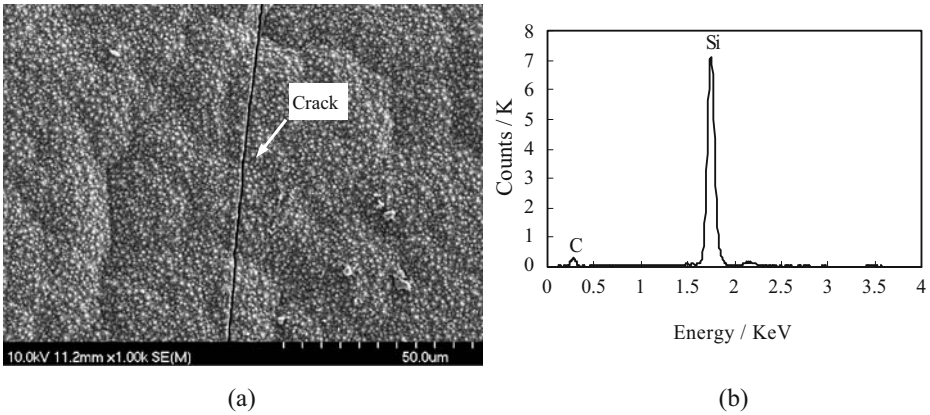

Fig. 5 Characterization of the SiC-B_4C coating oxidized at 700°C for 100 h showing, **a** surface morphology, **b** EDS pattern

of water in vitreous silica is much larger than that of oxygen [26], these will result in a gradient distribution of water in the silica. The solution of water will significantly decrease the viscosity of silica. Then, it can be deduced that the external layer of silica has a bigger solution of water and a low viscosity, while the internal layer of silica has a smaller solution

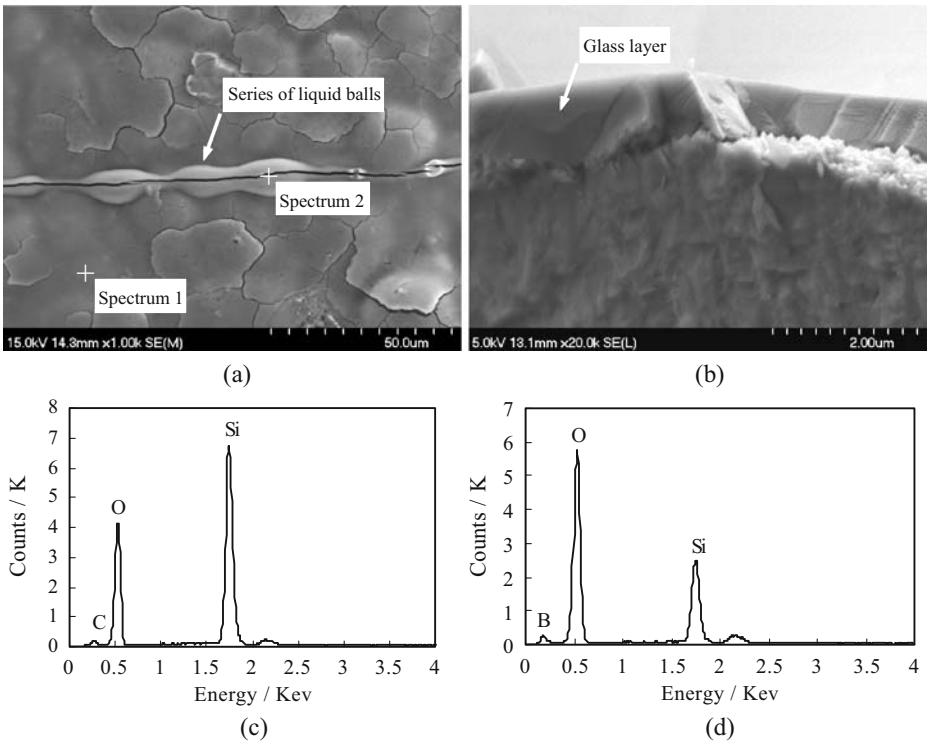

Fig. 6 Characterization of the SiC-B_4C coating oxidized at 1,000°C for 100 h showing, **a** surface morphology, **b** fracture section morphology, **c** EDS pattern of spectrum 1 in (**a**), **d** EDS pattern of spectrum 2 in (**a**)

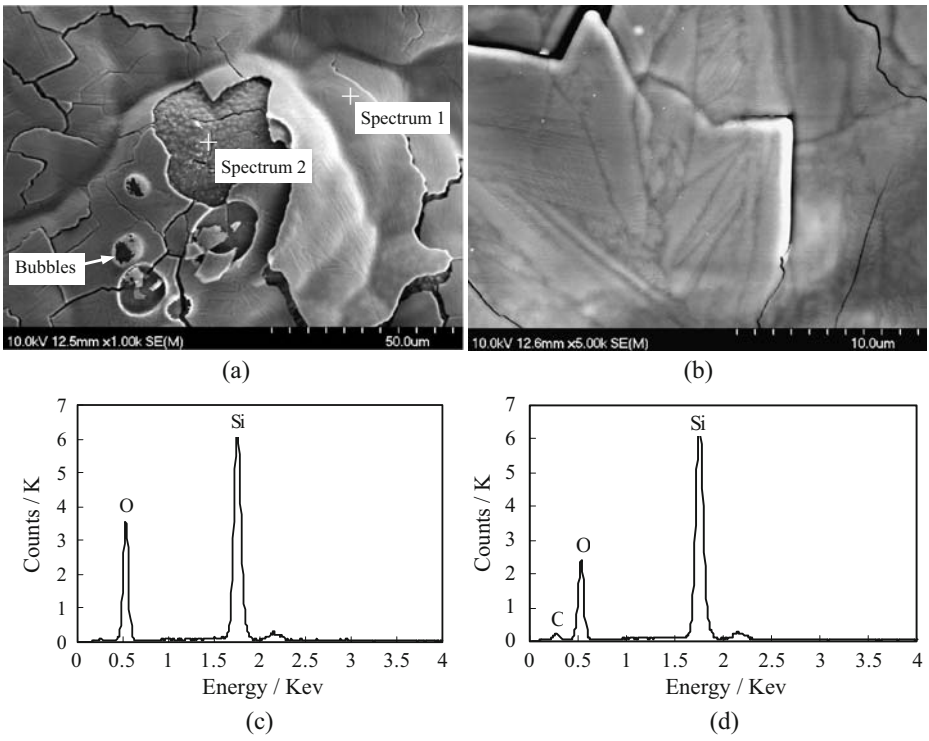

Fig. 7 Characterization of the SiC-B_4C coating oxidized at 1,200°C for 100 h showing, **a** surface morphology with low magnification, **b** surface morphology with high magnification, **c** EDS pattern of spectrum 1 in (**a**), **d** EDS pattern of spectrum 2 in (**a**)

of water and a high viscosity. Under oxidation at 1,200°C in wet environment, gaseous species will be produced. These gaseous products diffuse into the SiO_2 layer and form bubbles. The internal layer of silica has a high viscosity, and the bubbles are hard to escape, so the internal part of silica layer is porous. While the viscosity of external silica layer is low, bubbles will easily escape, thus the structure of external part of silica layer is dense.

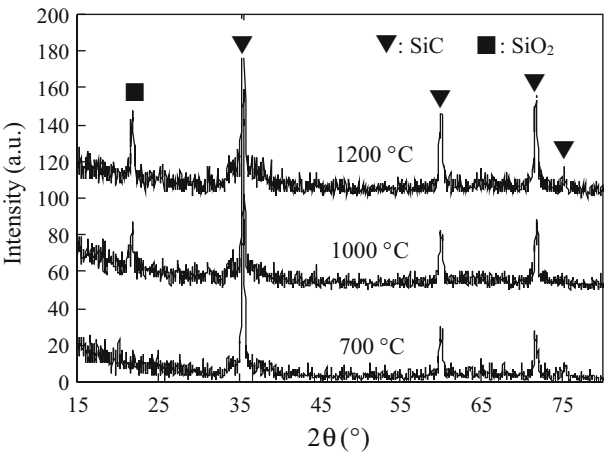

Fig. 8 GIXRD patterns of the SiC/B_4C coatings after oxidation for 100 h

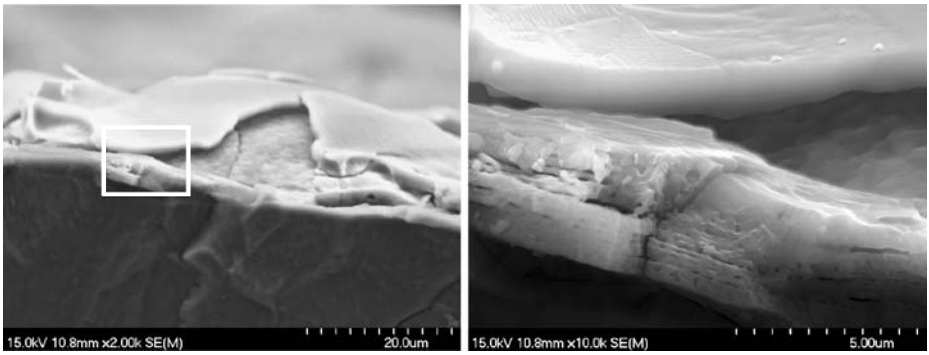

Fig. 9 Fracture section morphology of the SiC-B_4C coating after oxidation at 1,200°C for 100 h **a** morphology with low magnification, **b** morphology with high magnification

3.3 Weight Change of SiC-B_4C Coated C/SiC Composite

Figure 10 shows the weight changes of SiC-B_4C coating coated C/SiC composite after oxidation for 100 h. The weight changes of SiC-SiC coated C/SiC composite were also given for comparison. It can be seen that the SiC-B_4C coated C/SiC showed weight loss at 700°C, and weight gain above 1,000°C.

At 700°C, the SiC-B_4C coated C/SiC composite showed a parabolic weight loss for the initial 5 h, and then the weight loss got steadied for the next 20 h. After that the weight loss gradually accelerated, especially after oxidation for about 50 h. It can be deduced that during oxidation at 700°C, the liquid B_2O_3 can nearly seal the cracks within the initial 5 h. During the following 20 h, the oxidation is mainly controlled by diffusion of oxygen and water in liquid B_2O_3. The steadied weight change indicates that weight gain caused by oxidation of B_4C and weight loss caused by the evaporation of B_2O_3 and oxidation of carbon phase got balanced. While, with the evaporation of B_2O_3 carrying on, the seal of cracks got abated, and the oxidation of carbon phase was aggravated. So the weight loss gradually accelerated with time prolongs. Even though, the weight loss of SiC-B_4C coated

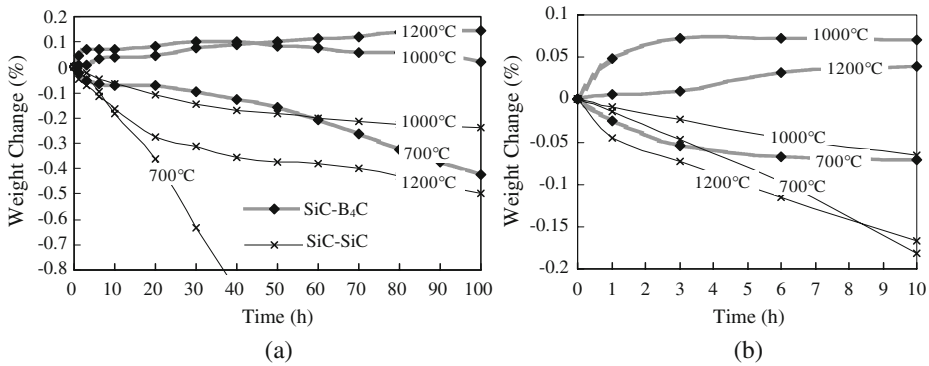

Fig. 10 Weight change of the coated 3D C/SiC composite **a** oxidized for 100 h, **b** detailed information for initial 10 h of (**a**)

C/SiC after oxidized at 700°C for 100 h is about 0.45%, which is much smaller than that of SiC-SiC coated C/SiC.

At 1,000°C, the SiC-B_4C coated C/SiC showed that the weight increased rapidly for the initial 3 h, and then the weight almost kept steady. It can be deduced that at 1,000°C, the breadth of cracks was reduced and the formation of B_2O_3 was accelerated, so it is easier to seal cracks. Meanwhile the oxidation of SiC resulted in a thin layer SiO_2 and the formation of SiO_2 would be significantly increase by B_2O_3 [27]. While, the SiC-SiC coated C/SiC can only seal cracks by the formation of SiO_2, which is slow at this condition.

At 1,200°C, the SiC-B_4C coated C/SiC showed approximate linear weight gain. At this temperature, the oxidation of SiC was enhanced by B_2O_3 and water [26, 27]. Also, B_2O_3 and SiO_2 would combine to form boron silicate, and the saturated vapor pressure of boron silicate is much lower than that of B_2O_3, which means that the evaporation of B_2O_3 was slowed down. The enhanced oxidation of SiC and the weakened evaporation of B_2O_3 resulted in the linear weight gain of SiC-B_4C coated C/SiC at 1,200°C.

3.4 Residual Flexural Strength of SiC-B_4C Coated C/SiC Composite

The residual flexural strength of coated C/SiC after oxidation at 700°C, 1,000°C and 1,200°C for 100 h was compared as shown in Fig. 11. The residual strength of the SiC-B_4C coated C/SiC is higher than that of SiC-SiC coated C/SiC below 1,000°C, especially at 700°C, the residual strength of the SiC-SiC coated C/SiC is about 64%, while that of SiC B_4C coated C/SiC is about 86%. After oxidized at 1,000°C, the residual strength of SiC-B_4C coated C/SiC was almost constant, while a small strength loss (94% retained strength) was achieved by SiC-SiC coated C/SiC. After oxidized at 1200°C, the residual strength of the SiC-B_4C coated C/SiC (86%) is slightly lower than that of SiC coated C/SiC (89%). These results indicated that compared with SiC-SiC coating, the SiC-B_4C hybrid coating could provide better protection for C/SiC composite in $P_{H_2O}/P_{O_2}/P_{Ar} = 14/8/78$ atmosphere for 100 h up to 1,000°C.and the protection of SiC-B_4C coating is still efficient at 1,200°C.

4 Conclusions

1. The crack density of SiC-B_4C hybrid coating was about half of that of SiC coating. Due to the less adhesion at the heterogeneous interfaces of the SiC-B_4C coating, which not only release thermal stress but also weaken transfer of the thermal stress.

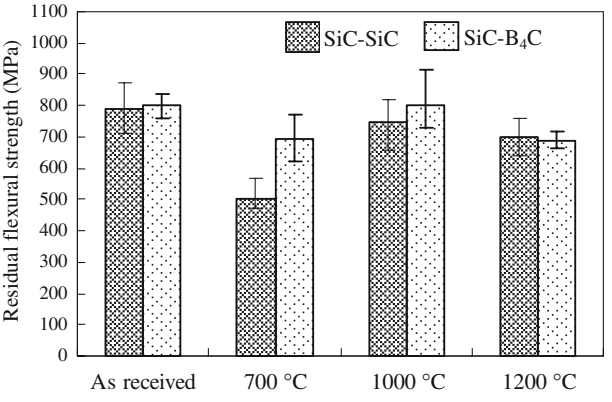

Fig. 11 Residual flexural strength of the coated C/SiC before and after oxidation for 100 h

2. Wet oxidation behaviors of C/SiC composite protected by SiC-B_4C coating and SiC-SiC coating were investigated in an environment of $P_{H_2O}/P_{O_2}/P_{Ar} = 14/8/78$ at 700°C, 1,000°C and 1,200°C for 100 h. The SiC-B_4C coated C/SiC showed much smaller weight loss at 700°C than that of SiC-SiC coated C/SiC. Above 1,000°C, the SiC-B_4C coated C/SiC showed a slight weight gain, while SiC-SiC coated C/SiC showed weight loss.
3. The residual strength analysis indicated that the SiC-B_4C coating was more efficient to protect C/SiC than that of SiC-SiC coating below 1,000°C, especially at 700°C, the residual strength of SiC-B_4C coated C/SiC is about 86%., while that of the SiC-SiC coated C/SiC is about 64%. The residual strength of the SiC-B_4C coated C/SiC (86%) is slightly lower than that of SiC coated C/SiC (89%) after oxidation at 1,200°C. The SiC-B_4C coating can provide C/SiC composite in wet oxygen atmosphere up to 1,200°C for 100 h.

Acknowledgments The authors acknowledge the support of the National Basic Research Program of China

References

1. Cox, B.N., Zok, F.W.: Solid State. Mater. Sci. **1**, 666 (1996)
2. Halbig, M.C., Brewer, D.N., Eckel, A.J.: New York: NASA (1997). NASA/TM-1997-107457
3. Naslain, R.: Compos. Sci. Technol. **64**, 155 (2004). doi:10.1016/S0266-3538(03)00230-6
4. Naslain, R. (ed.): T. Cutard, M. Huger, D. Fargeot: Proc of HT–CMC1, pp 33–49. Woodhead, Abington Cambridge (1993)
5. Schmidt, S., Beyer, S., Knabe, H., Immich, H., Meistring, R., Gessler, A.: Acta Astronaut. **55**, 409 (2002). doi:10.1016/j.actaastro.2004.05.052
6. Cheng, L.F., Xu, Y.D., Zhang, L.T., Yin, X.W.: J. Mater. Sci. **37**, 5339 (2002). doi:10.1023/A:1021089411141
7. Strife, J.R., Sheehan, J.E.: Ceram. Bull. **67**, 369 (1988)
8. Liu, Y.S., Cheng, L.F., Zhang, L.T., Wu, S.J., Li, D.: Mater. Sci. Eng. A **46**, 172 (2007). doi:10.1016/j.msea.2007.02.059
9. Naslain, R., Guette, A., Rebillat, F., Pailler, R., Langlais, F., Bourrat, X.: J. Solid State Chem. **177**, 449 (2004). doi:10.1016/j.jssc.2003.03.005
10. Lamouroux, F., Bertrand, S., Pailler, R., Naslain, R., Cataldi, M.: Compos. Sci. Technol. **59**, 1073 (1999). doi:10.1016/S0266-3538(98)00146-8
11. Wu, S.J., Cheng, L.F., Yang, W.B., Liu, Y.S., Zhang, L.T., Xu, Y.D.: Appl. Compos. Mater. **13**, 397 (2006). doi:10.1007/s10443-006-9025-8
12. Jacques, S., Guette, A., Langlais, F., Naslain, R.: J. Mater. Sci. **32**, 983 (1997). doi:10.1023/A:1018570120680
13. Quemard, L., Rebillat, F., Guette, A., Tawil, H., Pouillerie, C.L.: J. Eur. Ceram. Soc. **27**, 2085 (2006). doi:10.1016/j.jeurceramsoc.2006.06.007
14. Viricelle, J.P., Goursat, P., Bahloul-Hourlier, D.: Compos. Sci. Technol. **61**, 607 (2001). doi:10.1016/S0266-3538(00)00243-8
15. Carrère, P., Lamon, J.: J. Eur. Ceram. Soc. **23**, 1105 (2003). doi:10.1016/S0955-2219(02)00273-X
16. Schulte-Fischedicka, J., Schmidtb, J., Tammea, R., Krönera, U., Arnolda, J., Zeiffera, B.: Mater. Sci. Eng. A **386**, 428 (2004)
17. Rebillat, F., Martin, X., Guette, A.: Proceedings of High Temperature Ceramic Matrix Composites 5 (HTCMC 5), p 321. The Am. Ceram. Soc., Westerville, Ohio, USA (2004)
18. Quemard, L., Martin, X., Rebillat, F., Guette, A.: Proceedings of High Temperature Ceramic Matrix Composites 5 (HTCMC 5), p 327. The Am. Ceram. Soc., Westerville, Ohio, USA (2004)
19. Jacobson, N., Farmer, S., Moore, A., Sayir, H.: J. Am. Ceram. Soc. **82**, 393 (1999)
20. Jacobson, N.S.: J. Am. Ceram. Soc. **76**, 3 (1993). doi:10.1111/j.1151-2916.1993.tb03684.x
21. Berjonneau, J., Chollon, G., Langlais, F.: J. Electrochem. Soc. **153**, 795 (2006). doi:10.1149/1.2353566
22. Berjonneau, J., Langlais, F., Chollon, G.: Sur. Coat. **516**, 2848 (2008)
23. Sheehan, J.E.: Carbon **27**, 709 (1989). doi:10.1016/0008-6223(89)90204-2
24. Opila, E.J.: J. Am. Ceram. Soc. **77**, 730 (1994). doi:10.1111/j.1151-2916.1994.tb05357.x
25. Opila, E.J.: J. Am. Ceram. Soc. **82**, 625 (1999)
26. Deal, B.E., Grove, A.S.: J. Appl. Phys. **36**, 3770 (1965). doi:10.1063/1.1713945
27. Schlichting, J.: High Temp. High Press. **14**, 717 (1982)